

# Weak gravitational lensing by fourth order gravity black holes

Zsolt Horváth\* and László Á. Gergely†

*Departments of Theoretical and Experimental Physics,  
University of Szeged, Dóm tér 9, Szeged 6720, Hungary*

David Hobill‡

*Department of Physics and Astronomy, University of Calgary, Calgary Alberta T2N 1N4, Canada*

Salvatore Capozziello§ and Mariafelicia De Laurentis¶

*Dipartimento di Scienze Fisiche, Università di Napoli “Federico II”, Napoli, Italy  
INFN Sez. di Napoli, Compl. Univ. di Monte S. Angelo, Edificio G, Via Cinthia, I-80126, Napoli, Italy*

We discuss weak lensing characteristics for black holes in a fourth order  $f(R)$  gravity theory, characterized by a gravitational strength parameter  $\sigma$  and a distance scale  $r_c$ . Above  $r_c$  gravity is strengthened and as a consequence weak lensing features are modified compared to the Schwarzschild case. We find a critical impact parameter (depending upon  $r_c$ ) for which the behavior of the deflection angle changes. Using the Virbhadra-Ellis lens equation we improve the computation of the image positions, Einstein ring radii, magnification factors and the magnification ratio. We demonstrate that the magnification ratio as function of image separation has a different power-law dependence for each parameter  $\sigma$ . As these are the lensing quantities most conveniently determined by direct measurements, future lensing surveys will be able to constrain the parameter  $\sigma$  based on this prediction.

PACS numbers: 95.30.Sf, 04.50.Kd, 98.62.Sb

## I. INTRODUCTION

The recent advent of the so-called “Precision Cosmology” along with galactic observations indicate that General Relativity (GR) with standard matter sources disagrees with an increasing number of observational data, e. g. those coming from IA-type Supernovae, used as standard candles, large scale structure ranging from galaxies up to super-clusters [1–3], and galactic rotation curves. In addition, from a theoretical point of view, being not renormalizable, GR fails to be quantized in any *standard* way (see [4]). Therefore from ultra-violet up to infrared scales GR is not and cannot be the definitive theory of Gravitation despite the fact that it successfully addresses a wide range of phenomena and the Newtonian weak field limit is correctly recovered.

In order to interpret the recent observational data in the framework of GR, the introduction of unknown *dark matter* (DM) (to address dynamical phenomena as the formation of self-gravitating astrophysical structures) and *dark energy* (DE) (to address the problem of cosmic acceleration) seems to be necessary: however, the price of preserving the simplicity of the Hilbert-Einstein Lagrangian has been the introduction of rather odd-behaving physical entities that, up to now, have not been revealed by any experiment at fundamental scales. This situation has led to several attempts devoted either to recover the validity of GR at any scale, or to construct alternative gravity theories that suitably generalize the Einsteinian one. The philosophy of these two schemes is that in the former case one has to modify the matter sector introducing DM and DE, in the latter approach the dynamics of the geometry (i.e. the left-hand-side of the Einstein equations) is modified but with the constraint to recover GR at local scales.

Higher-order theories of gravity (both in metric [5–9] and Palatini [10–12] formulations) represent an interesting approach able to fruitfully cope with both dark matter and dark energy problems. A further approach is based on scalar-tensor theories of gravity but it can be shown that higher-order theories and scalar tensor ones can be related by conformal transformations (see, e.g., [6, 13] and references therein).

It has been widely demonstrated that such theories can agree with the cosmological observations of the Hubble flow [14, 15] and the large scale structure evolution [16]. In addition, in the weak field limit, the gravitational potential

---

\*Electronic address: zshorvath@titan.physx.u-szeged.hu

†Electronic address: gergely@physx.u-szeged.hu

‡Electronic address: hobill@ucalgary.ca

§Electronic address: capozzie@na.infn.it

¶Electronic address: felicia@na.infn.it

turns out to be modified [17–20] in such a way that interesting consequences to galactic dynamics may be achieved without violating, at the same time, the constraints on the parametrized post-Newtonian (PPN) parameters coming from Solar System tests [21].

If alternative theories of gravitation are able to explain both cosmological and local observations without the introduction of exotic energy-momentum sources, then one might ask how would the differences between these alternative theories be compared to GR with the unusual sources? It is proposed that gravitational lensing might be able to act a means for determining which theory governs the gravitational interaction, through measurements of image separations and the brightnesses of those multiple images.

It is well known that the deflection of light observed during the Solar eclipse of 1919 was one of the first experimental confirmations of Einsteinian GR. *Gravitational lensing*, i.e. the deflection of light rays crossing the gravitational field of a compact object referred to as the *lens*, has become one of the most astonishing successes of GR and it represents nowadays a powerful tool capable of putting constraints on the dynamics of gravitational structures at different scales, from stars to galaxies and clusters of galaxies, and from the large scale structure to cosmological parameters [22, 23]. If we modify the Lagrangian of the gravitational field, it is obvious that gravitational lensing should be affected. It is therefore mandatory to investigate how gravitational lensing behaves in the framework of alternative theories of gravity to develop a further check on the existence of DM and DE.

In particular, one has to verify that the phenomenology of standard gravitational lensing is recovered in the limit as the modified theory of gravity reduces to GR, since several observations point to the validity of GR. However, it is worth stressing that the presence of DM has to be invoked in such cases, in particular for large-scale structure (see e.g. the case of Bullet Cluster [24]). On the other hand, it is worth exploring whether deviations from the classical results for the main lensing quantities could be detected and act as clear signatures for modified theories of gravity.

As a first step towards such an ambitious task we consider here power-law fourth order theories, i.e. we replace the Ricci scalar  $R$  in the gravity Lagrangian with the function  $f(R) \propto R^n$  (with  $n$  a positive integer) and investigate how this affects the gravitational lensing in the case of black hole solutions to the theory. In Ref. [25] the gravitational lensing in  $f(R)$  theories with a Yukawa-type correction in the potential was investigated and the conclusion reached was that weak lensing could not discern between these theories and general relativity. As an alternative, we will consider the weak lensing phenomenology for black hole space-time coming from  $R^n$ -gravity in which gravitational lensing can occur.

The paper is organized as follows. The next section provides a short summary of  $f(R)$  theories, focusing on the special  $R^n$  case. We will prove in Section III that the predictions of weak gravitational lensing are different in the fourth order theory and in general relativity. For this we determine the image locations, Einstein ring radii, magnification factors and the flux ratio, for various model parameters. We then prove that the flux ratio as function of image separation has a different power-law dependence for each model parameter. We summarize our findings in the Concluding Remarks.

## II. GENERALITIES OF $f(R)$ -GRAVITY

Let us consider now a particular class of higher order theories of gravity, the  $f(R)$ -gravity theories, that are the most natural extension of GR where the Hilbert-Einstein action is modified with a general function of the scalar curvature [5, 6]. A general action is:

$$\mathcal{A} = \int d^4x \sqrt{-g} [f(R) + \mathcal{L}_m] \quad (1)$$

where  $f(R)$  is a generic function of the Ricci curvature scalar  $R$ , differentiable at least up to the second order,  $g$  is the determinant of the metric and  $\mathcal{L}_m$  is the standard matter Lagrangian<sup>1</sup> Varying the action with respect to the metric components  $g_{\mu\nu}$ , one obtains the generalized field equations that can be recast as [9, 29]:

$$G_{\mu\nu} = \frac{1}{f'(R)} \left\{ \frac{1}{2} g_{\mu\nu} [f(R) - Rf'(R)] + f'(R)_{;\mu\nu} - g_{\mu\nu} \square f'(R) \right\} + \frac{T_{\mu\nu}^{(m)}}{f'(R)} \quad (2)$$

---

<sup>1</sup> It is possible to take into account also the Palatini approach in which the metric  $g$  and the connection  $\Gamma$  are considered independent fields (see for example [26]). Here we consider the Levi-Civita connection and use the metric approach. See [5, 27] for a detailed comparison between the two pictures.

where  $G_{\mu\nu} = R_{\mu\nu} - \frac{R}{2}g_{\mu\nu}$  and  $T_{\mu\nu}^{(m)}$  are the Einstein tensor and the standard matter stress-energy tensor, respectively. The prime denotes derivative with respect to  $R$ . The two terms  $f'(R)_{;\mu\nu}$  and  $\square f'(R)$  imply fourth order derivatives of the metric  $g_{\mu\nu}$  so that these models are also referred to as *fourth order gravity*. Starting from Eq. (2) and adopting the Robertson-Walker metric, it is possible to show that the Friedmann equations may still be written in the usual form provided that an *effective curvature fluid* (hence the name of *curvature quintessence*) is added to the matter term with energy density and pressure depending on the choice of  $f(R)$  [9].

The simplest choice for  $f(R)$  is a power-law like  $f(R) \propto R^n$  with  $n$  the slope of the Lagrangian (clearly, with  $n = 1$ , we recover the Einstein theory). In order to compare these power-law models with GR, we can search for spherically symmetric solutions of Eqs. (2) and then compute the Newtonian limit. One has to consider the gravitational field generated by a pointlike source and then solve the vacuum case. Under the hypotheses of a weak gravitational field and slow motion sources. In general, we can write the space-time metric as :

$$ds^2 = A(r)dt^2 - B(r)dr^2 - r^2d\Omega^2 \quad (3)$$

where  $d\Omega^2 = d\theta^2 + \sin^2\theta d\varphi^2$  is the line element on the unit sphere. It is worth noticing that the Birkhoff theorem does not hold for any  $f(R)$  but only for restricted classes of these models as discussed in details in [28].

To obtain the value of the two unknown functions  $A(r)$  and  $B(r)$ , we take the 00-vacuum component and the trace of the field equations (2) in the absence of matter :

$$3\square f'(R) + Rf'(R) - 2f(R) = 0 ,$$

to get a single equation :

$$f'(R) \left( 3\frac{R_{00}}{g_{00}} - R \right) + \frac{1}{2}f(R) - 3\frac{f'(R)_{;00}}{g_{00}} = 0 . \quad (4)$$

Eq. (4) is completely general and holds for any function  $f(R)$ . Note that even if the metric is stationary so that  $\partial_t g_{\mu\nu} = 0$ , the term  $f'(R)_{;00}$  is not vanishing because of the existence of non-zero Christoffel symbols entering the covariant derivatives. With the above power-law choice for the  $f(R)$ -Lagrangian, Eq. (4) reduces to :

$$R_{00}(r) = \frac{2n-1}{6n} A(r)R(r) - \frac{n-1}{2B(r)} \frac{dA(r)}{dr} \frac{d \ln R(r)}{dr} , \quad (5)$$

while the trace equation reads :

$$\square R^{n-1}(r) = \frac{2-n}{3n} R^n(r) . \quad (6)$$

Note that as soon as  $n = 1$ , Eq. (6) reduces to  $R = 0$ , which, when inserted into Eq. (5), gives  $R_{00} = 0$  and then the standard Schwarzschild solution is recovered. In general, expressing  $R_{00}$  and  $R$  in terms of the metric (3), Eqs. (5) and (6) become a system of two nonlinear coupled differential equations for the two functions  $A(r)$  and  $B(r)$ . A physically motivated hypothesis is to search for (Schwarzschild-like) solutions of the form

$$A(r) = \frac{1}{B(r)} = 1 + \frac{2\Phi(r)}{c^2} , \quad (7)$$

where  $\Phi(r)$  is the gravitational potential at the distance  $r$  from a pointlike mass  $m$ .

With these hypotheses, the vacuum field equations reduce to a system of two differential equations in the only unknown function  $\Phi(r)$ . To be more precise, we can solve Eq. (5) or (6) to determine  $\Phi(r)$  and then use the other relation as a constraint to obtain solutions of physical interest.

A general exact black hole solution is

$$\Phi(r; \sigma, r_c) = -\frac{Gm}{2r} \left[ 1 + \left( \frac{r}{r_c} \right)^\sigma \right] , \quad (8)$$

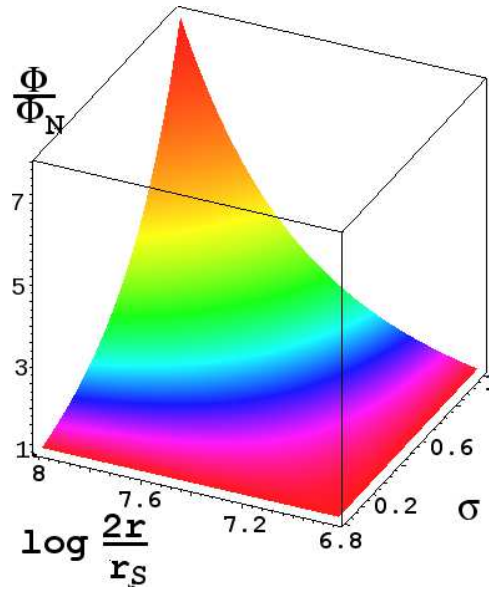


FIG. 1: The ratio of the power-law  $f(R)$  gravitational potential and the Newtonian gravitational potential as a function of  $\sigma \in [0, 1)$  and of the logarithm of the distance  $r \geq r_c$ , normalized to  $r_S$  (the Schwarzschild radius of the lens). We have chosen a typical bulge mass of  $10^{10} M_\odot \approx 2 \times 10^{40}$  kg and  $r_c \approx r_{bulge} \approx 10^{20}$  m.

where the gravitational potential differs from the standard Newtonian one due to the second term on the right hand side [29], containing the parameter  $\sigma$  and a characteristic distance  $r_c$ . It is straightforward to see that, for  $\sigma = 0$ , the Newtonian potential is recovered and the metric reduces to the Schwarzschild one (GR-case). We exclude the cases  $\sigma > 1$  (as the correction to the Newtonian potential asymptotically diverges) and  $\sigma = 1$  (as the correction is a constant, obstructing asymptotic flatness).

To check the validity of solution (8), we insert the expression for  $\Phi(r)$  into Eqs. (5) and (6), which both reduce to algebraic equations and are solved to obtain :

$$(n-1)(\sigma-3) [-\sigma(1+\sigma)V_1\eta^{\sigma-3}]^{n-1} \left[ 1 + \frac{\sigma V_1 \mathcal{P}_0}{\mathcal{P}_1 \eta} \right] \mathcal{P}_1 \eta = 0, \quad (9)$$

where  $\eta = r/r_c$ ,  $V_1 = Gm/c^2 r_c$  and

$$\mathcal{P}_0 = 3(\sigma-3)^2 n^3 - (5\sigma^2 - 31\sigma + 48)n^2 - (3\sigma^2 - 16\sigma + 17)n - (\sigma^2 - 4\sigma - 5), \quad (10)$$

$$\mathcal{P}_1 = 3(\sigma-3)^2(1-\sigma)n^3 + (\sigma-3)^2(5\sigma-7)n^2 - (3\sigma^3 - 17\sigma^2 + 34\sigma - 36)n + (\sigma^2 - 3\sigma - 4)\sigma. \quad (11)$$

Eq. (9) is identically satisfied for particular values of  $n$  and  $\sigma$ . It should be noted that when deriving Eq. (5) from Eq. (4), we assumed  $R \neq 0$ , which eliminates the case  $n = 1$ . Secondly,  $\sigma = 3$  may also be rejected since as noted above, all  $\sigma > 1$  lead to divergences. The third factor cannot vanish as it would imply either  $\sigma = 0$  or  $\sigma = -1$  for which  $n$  is less than unity.

We can then look for further solutions of Eq. (9) solving

$$\mathcal{P}_1(n, \sigma)\eta + \sigma V_1 \mathcal{P}_0(n, \sigma) \simeq \mathcal{P}_1(n, \sigma)\eta = 0. \quad (12)$$

We neglected the second term of Eq. (12) since for large scale-lengths  $r_c$  the parameter  $V_1 \ll 1$  and both  $n$  and  $\sigma$  are of order unity. Eq. (12) is an algebraic equation for  $\sigma$  as function of  $n$  with the following three solutions :

$$\sigma = \begin{cases} \frac{3n-4}{n-1} \\ \frac{12n^2-7n-1-\sqrt{p(n)}}{q(n)} \\ \frac{12n^2-7n-1+\sqrt{p(n)}}{q(n)} \end{cases} \quad (13)$$

with :

$$p(n) = 36n^4 + 12n^3 - 83n^2 + 50n + 1 ,$$

and

$$q(n) = 6n^2 - 4n + 2 .$$

It is easy check that, for  $n = 1$  the second solution (13) gives  $\sigma = 0$ , i.e. the second approximate solution reduces to the Newtonian one as expected. As a final check, we have to insert back into the vacuum field Eqs. (4) and (6) the modified gravitational potential (8) with:

$$\sigma = \frac{12n^2 - 7n - 1 - \sqrt{36n^4 + 12n^3 - 83n^2 + 50n + 1}}{6n^2 - 4n + 2} . \quad (14)$$

The dependence of  $\sigma$  upon the exponent  $n$  is represented in Fig. 2

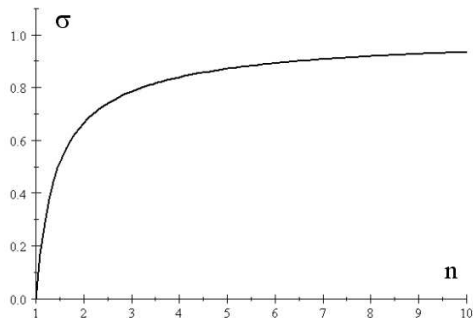


FIG. 2: The dependence of correction parameter  $\sigma$  in the potential upon the exponent  $n$ .

In the case  $n = 1$  (implying  $\sigma = 0$ ) the potential reduces to the Newtonian  $\Phi_N$ , as expected. The potential also reduces to the Newtonian value at  $r = r_c$ . For smaller values of  $r$  gravity is weakened compared to the Newtonian values, while for  $r > r_c$  gravity is strengthened.

While the power  $\sigma$  of the correction term is a universal quantity (since it depends on the exponent  $n$  entering the gravity Lagrangian), the scale-length  $r_c$  is related to the integration constants that have to be set to solve the fourth order differential equations of the theory. The radius  $r_c$  can be considered as a further gravitational radius complementing the Schwarzschild radius, originating in the fact that we consider a fourth order theory (compared to the second order GR) and as such it introduces two further degrees of freedom of the gravitational field. We expect  $r_c$  to be related to the peculiarities of each gravitational system. Therefore it can take different values depending upon the system's mass and typical length scale.

The fact that gravity is strengthened above  $r_c$  is illustrated in Fig. 1 by plotting the ratio of the potentials  $\Phi(r; \sigma, r_c) / \Phi_N(r)$  as function of  $\sigma$  and  $r$  for the ranges  $0 \leq \sigma < 1$  and  $r \geq r_c$  with a suitably chosen value of  $r_c$ . In the case of a typical spiral galaxy we identify  $r_c$  with the bulge radius  $r_{bulge}$ . If we choose, for example, mass of the bulge as  $10^{10} M_\odot \approx 2 \times 10^{40}$  kg, we find  $r_c \approx r_{bulge} \approx 10^{20}$  m. Therefore gravity is strengthened outside  $r_{bulge}$  as compared to the Newtonian case, providing an alternative to dark matter as a source for a flat rotation curve [30].

### III. WEAK LENSING IN FOURTH ORDER GRAVITY

#### A. The lensing geometry

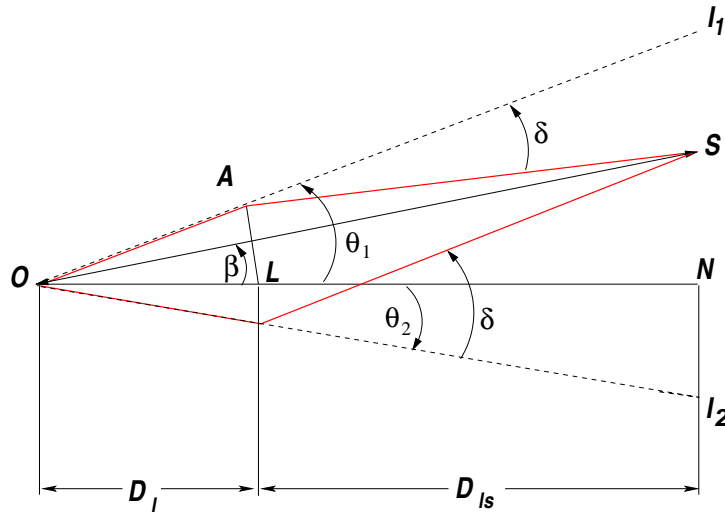


FIG. 3: The lensing geometry (see text for discussion of the symbols). Positive angles are represented with counterclockwise directed arcs.

The lensing geometry is shown on Fig. 3. The optical axis  $OLN$  is defined by the observer position  $O$ , the lens position  $L$ , and intersects the source plane at  $N$ . In the source plane  $S$  represents the location of the source and  $I_{1,2}$  the locations of the two images. We use the notations  $D_{ls}$  and  $D_l$  for the projection of the lens-source and observer-lens distances onto the optical axis respectively [31]. The observer-source distance is  $D_s = D_l + D_{ls}$ . The source is located at an angle  $\beta$  from the optical axis, chosen to be “above” the optical axis. Images are located at angles  $\theta_{1,2}$  with respect to the optical axis and they can be either positive (for the image above the optical axis) or negative (for the image below the optical axis). For either of the images we denote  $s = \text{sgn } \theta$ , such that  $|\theta| = s\theta$ . We follow the convention that the deflection angle is  $\delta > 0$  whenever the light is bent towards the optical axis, cf. Ref. [32]. Similarly as in Ref. [31], we characterize the mass by the dimensionless parameter  $\bar{\varepsilon} = Gm/c^2L$ , with  $L = D_s D_l / D_{ls}$ .

In Ref. [29] the leading order lens equation

$$|\theta| - s\beta - \frac{D_{ls}}{D_s} \delta = 0 \quad (15)$$

was employed for the discussion of the weak lensing. We increase the accuracy of the weak lensing analysis by applying here the Virbhadra-Ellis lens equation

$$\tan |\theta| - \tan (s\beta) - \frac{D_{ls}}{D_s} [\tan |\theta| + \tan (\delta - |\theta|)] = 0. \quad (16)$$

We compare the two approaches by computing the difference between the Einstein angles (defined as  $\theta_1 = \theta_2$ , occurring when  $\beta = 0$ ) obtained from Eqs. (15) and (16), respectively, as a function of the fourth order black hole parameter  $\sigma$  and mass parameter  $\bar{\varepsilon}$ . The results are shown in Fig 4.

#### B. The deflection angle

In Ref. [29] weak lensing by point-like  $f(R)$  black holes characterized by the potential (8) was investigated. A deflection angle

$$\delta = \frac{2Gm}{c^2 b} \left[ 1 + \frac{\sqrt{\pi}(1-\sigma)\Gamma(1-\sigma/2)}{2\Gamma(3/2-\sigma/2)} \left( \frac{b}{r_c} \right)^\sigma \right] \quad (17)$$

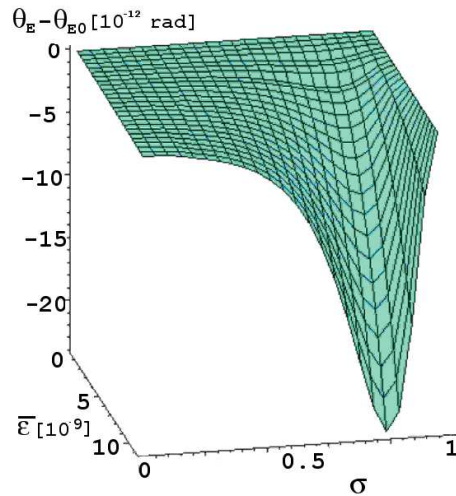


FIG. 4: The difference between the Einstein angles  $\theta_E$ , obtained from Eq. (16) and  $\theta_{E0}$ , obtained from Eq. (15), as function of the parameters  $\sigma$  and  $\bar{\epsilon}$ . We set the distances  $D_l = 1$  Mpc and  $D_{ls} = 2$  Mpc.

was derived, with  $b = \theta D_l$  the impact parameter (defined as the distance of the lensing object to the straight line trajectory, which would occur in the absence of the lensing object). For  $\sigma = 0$  the deflection angle reproduces the Schwarzschild value  $\delta_S = 4Gm/c^2b$ , while in the limit  $\sigma \rightarrow 1$  the deflection angle is one half of  $\delta_S$ .

In order to investigate the behavior of  $\delta$  in between the limiting values, we represent the deflection angle as function of  $\sigma$  in Fig. 5. Three conclusions stand out: i) by increasing the impact parameter at any fixed value of  $\sigma$ , the deflection angle always decreases, as in the Schwarzschild case; ii) there is a critical value of the ratio  $b/r_c$  at  $(b/r_c)_{crit} = 2$ , below which the deflection angle monotonically decreases with increasing  $\sigma$ , and above which there is a single maximum at some  $\sigma_{\delta_{max}}$ ; iii) the parameter value  $\sigma_{\delta_{max}}$  increases with the value of  $b/r_c$ . The rate of decrease of  $\delta$  with increasing  $b$  is lessened as compared to the Schwarzschild case for small impact parameters of order  $r_c$ .

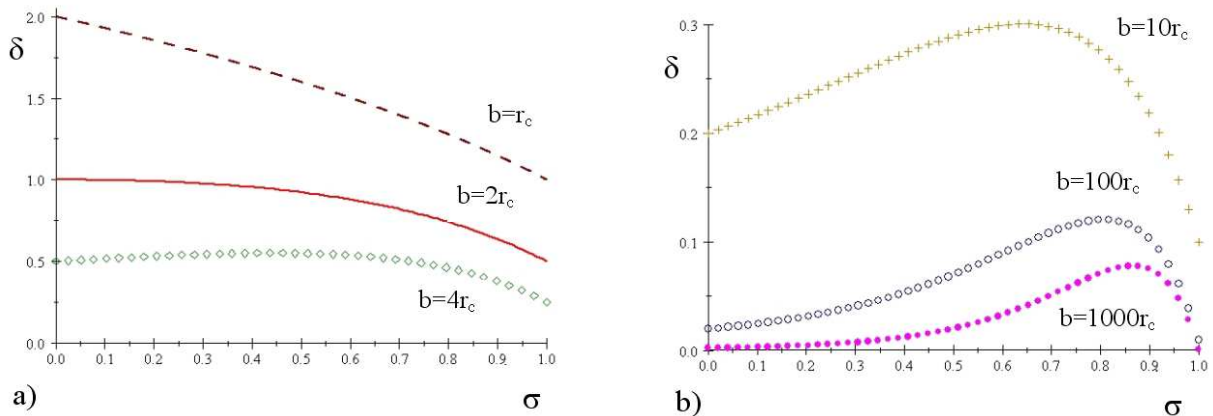


FIG. 5: The plots show the  $\delta(\sigma)$  dependence for different values of  $b/r_c$ , in units  $2Gm/c^2r_c = 1$ . The respective values of  $b/r_c$  are from top to bottom 1 (dashed), 2 (solid), 4 (diamond) on panel-a and 10 (cross), 100 (circle), 1000 (dotted) on panel-b. The critical behavior appears at  $b/r_c = 2$ .

### C. Image positions and magnifications

In Ref. [29] the image positions, the radius of the Einstein ring, image magnifications and the Paczynski curve in microlensing experiments were also estimated. In this follow-up paper we improve on the accuracy of the weak lensing

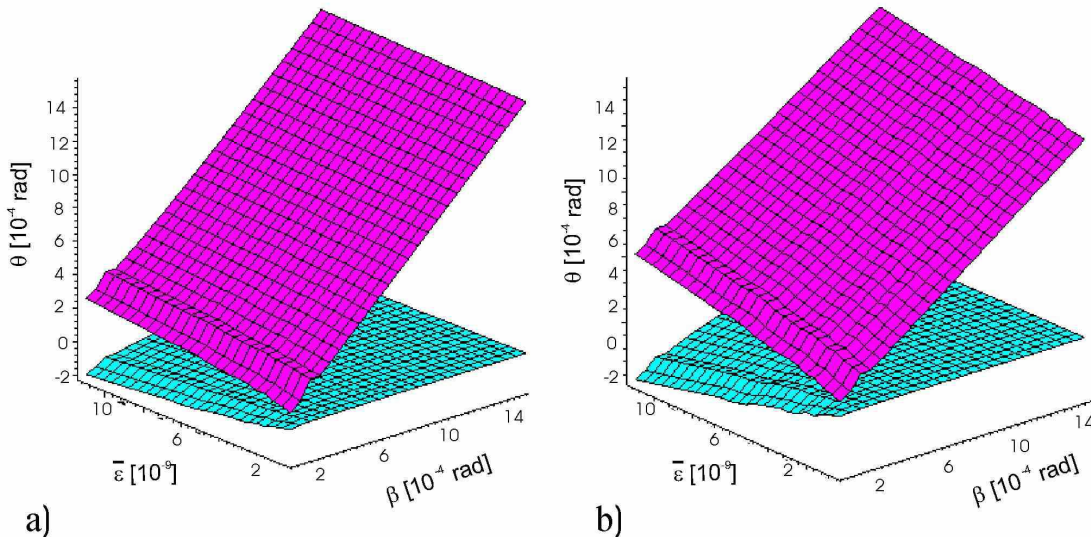


FIG. 6: The image positions  $\theta$  as function of  $\bar{\epsilon}$  and  $\beta$  for  $\sigma = 0.25$  (left) and  $\sigma = 0.75$  (right), for the distances  $D_l = 1$  Mpc and  $D_{ls} = 2$  Mpc. The angle  $\beta$  is varied up to 0.0015 rad, similarly as on Fig 4b of Ref. [31]. With decreasing  $\beta$ , the image separations shrink accordingly. At  $\beta = 0$  the angle  $\theta$  represents the angular radius of the Einstein ring. As we expect the  $\beta = 0$  sections of the surfaces are symmetric with respect to the plane  $\theta = 0$ .

characteristics, by employing a more accurate lens equation with the focus on the behavior of dimensionless observable quantities which can be derived from the image positions and magnification factors. Our task is to determine the measurable differences between the predictions of the fourth order theory and those of GR.

A weak lens equation was derived in Ref. [31] exclusively by trigonometric considerations and was applied to the computations of the image positions, magnifications and flux ratios to second order accuracy (both in the mass-related and tidal charge related small parameters) for brane-world black holes. It has been also shown, how the Virbhadr-Ellis lens equation follows as an approximation (agreement is reached in the first order of the perturbations). For the purposes of the present paper, not being concerned with second order effects, we will employ the Virbhadr-Ellis lens equation [32]-[34], together with the deflection angle (17) derived in Ref. [29]. This generalizes the approach of Ref. [29], where the leading order lens equation [Eq. (12) there] was employed for the discussion of weak lensing effects.

The numerical solution of the system of equations (17) and (16) gives the positions of the images as function of  $\bar{\epsilon}$  and  $\beta$ , represented on Fig. 6, for  $\sigma = 0.25$  and 0.75, respectively. In both cases decreasing  $\beta$  decreases the image separations. As expected, the  $\beta = 0$  sections give symmetric curves with respect to the planes  $\theta = 0$ . This is because at  $\beta = 0$  the angle  $\theta = \theta_E$  represents the angular radius of the Einstein ring. For small impact parameter (implying small  $\beta$ ) the image separations obey  $(\theta_1 - \theta_2)_{\sigma=0.25} < (\theta_1 - \theta_2)_{\sigma=0.75}$ , whereas for large values of  $\beta$  the image separations behave as  $(\theta_1 - \theta_2)_{\sigma=0.25} > (\theta_1 - \theta_2)_{\sigma=0.75}$ . This indicates that our analysis based on the Virbhadr-Ellis lens equation is more accurate than the first post-Newtonian order calculation performed in Section VIII. in Ref. [38], which states that  $f(R)$  gravity is indistinguishable from general relativity and is consistent with the observational value of the post-Newtonian parameter  $\gamma = 1 + (2.1 \pm 2.3) \times 10^{-5}$ .

The magnification of the images are defined as

$$\mu_{1,2} = \left| \frac{d\theta_{1,2}}{d\beta} \frac{\theta_{1,2}}{\beta} \right|. \quad (18)$$

For Schwarzschild lensing  $\mu_1 - \mu_2 = 1$  always holds. Fig 7 shows the image separations and magnifications as functions of  $\beta/\theta_E$  for  $\sigma = 0.25$  and 0.75. The upper and lower solid curves represent the primary and secondary image magnification factors, respectively; their ratio is the dashed curve; and the dotted curve is the image separation normalized with respect to the Einstein angle. The strongest effect appears on the ratio of magnifications, which



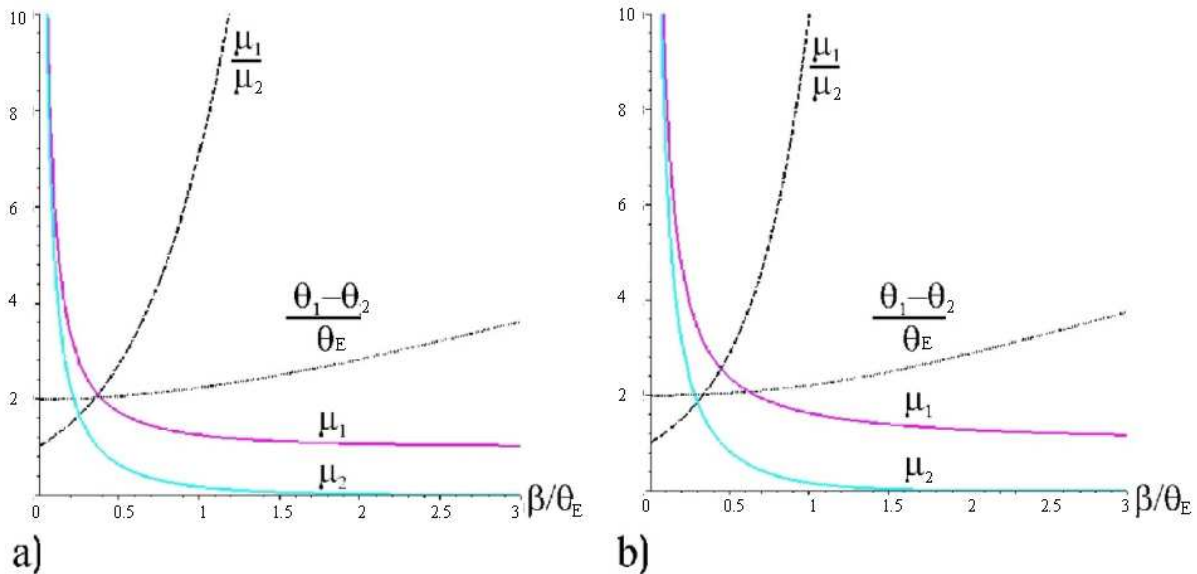


FIG. 7: The image separations and magnifications as functions of  $\beta/\theta_E$  for  $\sigma = 0.25$  (left) and  $\sigma = 0.75$  (right). We fixed  $\bar{\varepsilon} = 3.375 \times 10^{-9}$ , while the distances  $D_l = 1$  Mpc and  $D_{ls} = 2$  Mpc were chosen for the plots. The upper and lower solid curves represent the primary and secondary image magnification factors, respectively; their ratio is the dashed curve; and the dotted curve is the normalized image separation.

TABLE I: The different slopes  $\kappa$  of the curves indicate power law behaviours with different exponents for the various  $\sigma$ .

$\sigma$	0	0.25	0.5	0.75	0.9999
$\kappa$	6.8	7.3	7.55	7.7	8.1

increases more rapidly with  $\beta$  as  $\sigma$  increases. The reason for this is that the primary image is magnified more for larger values of  $\sigma$ .

#### D. Power-law behavior

In a lensing observation the most straightforward measurements are 1) the angular separation between the two images and 2) the ratio of the magnification factors. The first measurement does not require information on the location of the lens position, needed to define the individual image positions. The second measurement does not require an absolute measure of image brightness, since we are taking a ratio between the two.

Therefore we plot the ratio of the magnification factor for the primary and secondary images as function of the image separation (normalized to the Einstein angle), on the log-log scale, in Fig 8. The black (lowest) curve characterizes the lensing by a Schwarzschild black hole ( $\sigma = 0$ ), the colored curves, from bottom to top correspond to the fourth order gravity black hole lensing for the parameter values  $\sigma = 0.25, 0.5, 0.75$  and  $0.9999$ .

Similar to Ref. [31], for image separations greater than about 2.5 times the Einstein angle, the ratio of the magnification factors for each value of  $\sigma$  obeys a power-law relationship

$$\frac{\mu_1}{\mu_2} \propto \left( \frac{\Delta\theta}{\theta_E} \right)^\kappa. \quad (19)$$

The different slopes  $\kappa$  of the curves indicate power-law behaviors with different exponents, which are presented in Table I.

Given a large enough number of measurements of image separations and image brightnesses, these power-law relations provide an observational signature that can distinguish which among the fourth order  $f(R)$  theories with different  $\sigma$  (or  $n$ ) describes the black hole space-time.

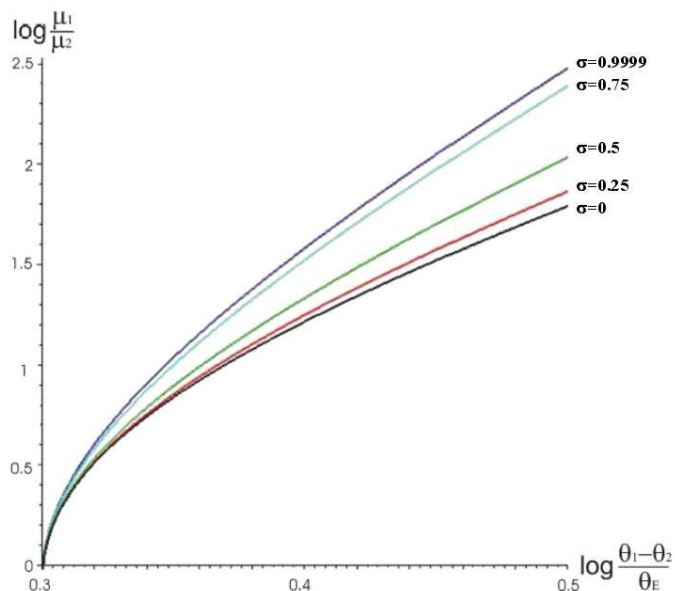


FIG. 8: The ratio of the magnification factor of the primary and secondary images as function of the image separation normalized to the Einstein angle, on the log–log scale for  $\sigma = 0., 0.25, 0.5, 0.75, 0.9999$ . We fixed  $\bar{\epsilon} = 3.375 \times 10^{-9}$ . We set the parameters  $D_l = 1$  Mpc,  $D_{ls} = 2$  Mpc. The different slopes of the curves indicate power-law behaviours with different exponents.

#### IV. CONCLUDING REMARKS

In this paper we have analyzed the weak lensing signatures of a fourth order ( $f(R) = R^n$ ) gravity black hole solution, with gravitational potential given by Eq. (8). This introduces a new parameter  $\sigma \in [0, 1)$ , which governs the deviation from the Newtonian gravitational potential. General relativity is contained as the special case  $n = 1$  (corresponding to the model parameter  $\sigma = 0$ ). A black hole in this theory generates a greater gravitational attraction at distances larger than  $r_c$  as compared to the prediction of Newtonian gravity.

Lensing properties of such black holes were analyzed before in Ref. [29], based on the small angle lens equation [34]. In this paper we have improved upon this approach, by employing the first order accurate Virbhadra-Ellis lens equation (16).

We analyzed the dependences upon  $\sigma$  and upon the impact parameter  $b$  of the deflection angle (17). The deflection angle decreases with increasing impact parameter for all  $\sigma$ . There is a transition at a critical value  $(b/r_c)_{crit} = 2$ , below which the deflection angle monotonically decreases with increasing  $\sigma$ , and above which there is a single maximum. This maximum value increases with the impact parameter.

The image positions as a function of the lensing mass and source position, also the image magnifications and their ratio as function of source position show features similar to those in the Schwarzschild case. Nevertheless, in contrast with previous claims in the literature, these lensing quantities depend upon  $\sigma$ .

We have computed the image positions for two values of  $\sigma$ . For the larger value of  $\sigma$ , the image separation grows faster with an increase in the mass and grows more slowly as the source moves away from the optical axis.

For the same source position the magnification factors of the images increase with  $\sigma$ , especially the one for the primary image. The increases in their ratio  $\mu_1/\mu_2$  is even more significant.

Using the most easily measurable lensing observables, the ratio of the magnifications is shown to have a power-law dependence on the image separations, with the power monotonically increasing with  $\sigma$ . This behavior provides a means for future gravitational lensing observations to either establish the value of  $\sigma$  or falsify the power-law gravitational potential discussed in this paper. Given that the next generation of radio telescopes will easily be able to resolve images to less than milli-arcsecond accuracy, the different rates at which the ratio of the magnifications changes should be able to provide a significant observational signature constraining the validity of  $f(R)$  gravitational theories.

## Acknowledgements

ZsH was supported by the European Union and co-funded by the European Social Fund through Grant No. TMOP 4.2.2/B-10/1-2010-0012. LG was partially supported by COST Action MP0905 "Black Holes in a Violent Universe" and by the Hungarian Scientific Research Fund (OTKA) grant no. 81364. DH acknowledges support from an NSERC Discovery Grant.

## References

- 
- [1] A. G. Riess et al., *AJ*, **116**, 1009 (1998); S. Perlmutter et al., *ApJ*, **517**, 565 (1999); R.A. Knop et al., *ApJ*, **598**, 102 (2003); J.L. Tonry et al., *ApJ*, **594**, 1 (2003); B.J. Barris et al., *ApJ*, **602**, 571 (2004); A.G. Riess et al., *ApJ*, **607**, 665 (2004).
- [2] P. de Bernardis et al., *Nature*, **404**, 955 (2000); A. Balbi et al., *ApJ*, **545**, 1 (2000); S. Hanany et al., *ApJ*, **545**, 5 (2000); T.J. Pearson et al., *ApJ*, **591**, 556 (2003).
- [3] C.L. Bennett et al., *ApJS*, **148**, 1 (2003); D.N. Spergel et al., *ApJS*, **148**, 175 (2003).
- [4] R. Utiyama, B S DeWitt, *J. Math. Phys.* **3**, 608 (1962).
- [5] S. Nojiri, S.D. Odintsov, *Int. J. Geom. Meth. Mod. Phys.* **4**, 115 (2007); S. Capozziello, M. Francaviglia, *Gen. Rel. Grav.* **40**, 357 (2008); S. Capozziello, M. De Laurentis, V. Faraoni, *The Open Astr. Jour.* **2**, 1874 (2009); T.P. Sotiriou, V. Faraoni, *Rev. Mod. Phys.* **82**, 451 (2010).
- [6] S. Capozziello, V. Faraoni, *Beyond Einstein Gravity: A Survey Of Gravitational Theories For Cosmology And Astrophysics*, Springer, New York (2010); S. Capozziello, M. De Laurentis, *Invariance Principles and Extended Gravity: Theory and Probes*, Nova Science Publishers, New York (2010).
- [7] S. Carloni, P.K.S. Dunsby, S. Capozziello, A. Troisi, *Class. Quant. Grav.* **22**, 4839 (2005); S. Capozziello, V.F. Cardone, A. Troisi, *Phys. Rev. D*, **71**, 043503 (2005).
- [8] S. Nojiri, S.D. Odintsov, *Phys. Lett. B*, **576**, 5 (2003); S. Nojiri, S.D. Odintsov, *Mod. Phys. Lett. A*, **19**, 627 (2003); S. Nojiri, S.D. Odintsov, *Phys. Rev. D*, **68**, 12352 (2003); S.M. Carroll, V. Duvvuri, M. Trodden, M. Turner, *Phys. Rev. D*, **70**, 043528 (2004).
- [9] S. Capozziello, *Int. J. Mod. Phys. D*, **11**, 483 (2002).
- [10] D.N. Vollick, *Phys. Rev. D*, **68**, 063510 (2003); X.H. Meng, P. Wang, *Class. Quant. Grav.*, **20**, 4949 (2003); E.E. Flanagan, *Class. Quant. Grav.*, **21**, 417 (2004); X.H. Meng, P. Wang, *Class. Quant. Grav.*, **21**, 951 (2004); G.M. Kremer, D.S.M. Alves, *Phys. Rev. D*, **70**, 023503 (2004).
- [11] S. Nojiri, S.D. Odintsov, *Gen. Rel. Grav.*, **36**, 1765 (2004); X.H. Meng, P. Wang, *Phys. Lett. B*, **584**, 1 (2004).
- [12] G. Allemandi, A. Borowiec, M. Francaviglia, *Phys. Rev. D*, **70**, 043524 (2004); G. Allemandi, A. Borowiec, M. Francaviglia, *Phys. Rev. D*, **70**, 103503 (2004).
- [13] V. Faraoni, *Cosmology in scalar-tensor gravity*, Kluwer Academic Publishers (2004).
- [14] S. Capozziello, V.F. Cardone, S. Carloni, A. Troisi, *Int. J. Mod. Phys. D*, **12**, 1969 (2003).
- [15] S. Capozziello, V.F. Cardone, M. Francaviglia, *Gen. Rel. Grav.* **38**, 711 (2006).
- [16] M. Amarzguoui, O. Elgaroy, D.F. Mota, T. Multamaki, *Astron. Astrophys.* **454**, 707 (2006) ; P. Zhang, *Phys. Rev. D* **73** 123504 (2006).
- [17] K.S. Stelle, *Gen. Rel. Grav.*, **9**, 353 (1978).
- [18] I. Quandt, H.J. Schmidt, *Astron. Nachr.*, **312**, 97 (1991).
- [19] P.D. Mannheim, *ApJ*, **419**, 150 (1993).
- [20] S. Capozziello, V.F. Cardone, S. Carloni, A. Troisi, *Phys. Lett. A*, **326**, 292 (2004).
- [21] S. Capozziello, M. De Laurentis, S. Nojiri, S.D. Odintsov *Gen. Rel. Grav.* **41**, 2313 (2009).
- [22] P. Schneider, J. Ehlers, E.E. Falco, *Gravitational lenses*, Springer-Verlag, Berlin (1992).
- [23] A.O. Petters, H. Levine, J. Wambsganss, *Singularity theory and gravitational lensing*, Birkhäuser, Boston (2001).
- [24] D. Clowe et al., *Astrophys. J.* **648** 109 (2006).
- [25] M. Lubini, C. Tortora, J. Näf, Ph. Jetzer, S. Capozziello, arXiv:1104.2851 (2011).
- [26] G. Magnano, M. Ferraris and M. Francaviglia, *Gen. Rel. Grav.* **19** 465 (1987).
- [27] S. Capozziello, M. De Laurentis, M. Francaviglia, S. Mercadante, *Found. Phys.* **39**, 1161 (2009) .
- [28] S. Capozziello, A. Stabile, A. Troisi *Phys. Rev. D* **76**, 104019 (2007).
- [29] S. Capozziello, V. F. Cardone, and A. Troisi, *Phys. Rev. D* **73** 104019 (2006). By replacing  $(\alpha, \beta, \xi)$  with  $(\delta, \sigma, b)$  we recover the notations of the present paper.
- [30] C. Frigerio Martins, P. Salucci, *Mon. Not. Roy. Astron. Soc.* **381**, 1103 (2007).
- [31] Z Horváth, L Á Gergely, D Hobill, *Class. Quant. Grav.* **27** 235006 (2010).
- [32] K S Virbhadra, *Phys. Rev. D* **79** 083004 (2009).
- [33] K S Virbhadra and G F R Ellis, *Phys. Rev. D* **62** 084003 (2000).

- [34] V Bozza, *Phys. Rev. D* **78** 103005 (2008).
- [35] S Capozziello, *Mon. Not. Roy. Astron. Soc.* **375** 1423 (2007).
- [36] P Schneider, *Astr. Ap.* **140** 119 (1984).
- [37] R Brandford, R Narayan, *Astroph. J.* **310** 568 (1986).
- [38] C P L Berry and J R Gair, *Phys. Rev. D* **83** 104022 (2011).